DOI: https://doi.org/10.15407/pmach2022.03.016

UDC 539.43

MULTI-CYCLE FATIGUE OF COMPOSITE THREE-LAYER PLATES WITH HONEYCOMB STRUCTURE MADE BY ADDITIVE FDM TECHNOLOGIES

[1] Borys V. Uspenskyi
Uspensky.kubes@gmail.com, ORCID: 0000-0001-6360-7430

[2] Ihor I. Derevianko
dereviankoii2406@gmail.com, ORCID: 0000-0002-1477-3173

[1, 3, 4] Kostiantyn V. Avramov
kvavramov@gmail.com, ORCID: 0000-0002-8740-693X

[1] Oleh F. Polishchuk
PolischukOleg@nas.gov.ua, ORCID: 0000-0003-1266-9847

[5] Oleksandr F. Salenko, ORCID: 0000-0002-5685-6225

[1] A. Pidhornyi Institute of Mechanical Engineering Problems of NASU, 2/10, Pozharskyi str., Kharkiv, 61046, Ukraine

[2] Yuzhnoye State Design Office, 3, Krivorizka str., Dnipro, 49008, Ukraine

[3] Kharkiv National University of Radio Electronics, 14, Nauky ave., Kharkiv, 61166, Ukraine

[4] National Aerospace University "Kharkiv Aviation Institute" 17, Chkalov str., Kharkiv, 61070, Ukraine

[5] National Technical University of Ukraine "Igor Sikorsky Kyiv Polytechnic Institute", 37, Peremohy ave., Kyiv, 03056, Ukraine

The multi-cycle fatigue of three-layer plates with honeycomb structure, which was manufactured using additive FDM technologies from polylactide, is considered. Carbon fiber based on the SIGRAPREG C U200-0/NF-E310/30% pre-preg is chosen as a material for the upper and lower covers. Fatigue analysis of three-layer plates with honeycomb structure is based on their vibration tests. To study the fatigue characteristics of honeycomb structures, special samples were made. Fatigue characteristics of structures are studied on three-layer samples using carbon-plastic sheathings. The experiment was accompanied by finite element simulation of fatigue tests in the ANSYS software complex. The fatigue properties of three-layer plates are studied.

***Keywords**: honeycomb structure, additive FDM technology, three-layer plates, fatigue tests, S-N curve.*

Introduction

The use of multi-layer thin-walled constructions with honeycomb structures is gaining popularity due to their rigidity, strength, and low weight. Such structural elements are used in satellites, rockets, airplanes, ships [1, 2]. Honeycomb structures have recently begun to be manufactured using additive technologies [3–5].

Several papers devoted to the fatigue characteristics of multi-layer samples have been published in the scientific literature. The paper [6] gives the results of the experimental analysis of three-layer plates with honeycomb structure and artificial defects. Fatigue characteristics of three-layer beams with honeycomb structures were experimentally studied using a four-point flexural test [7], and two types of samples (initially intact and damaged by delamination) were studied in this paper. The static and fatigue behavior of three-layer plates with front sides reinforced with aramid fibers and aluminum honeycomb structure was considered in the paper [8]. The effect of adhesion between front layers and honeycomb structure on the fatigue strength of a three-layer beam with aluminum honeycomb structure was studied in [9]. From the experiments, it follows that with an increase in adhesion, the fatigue strength increases. The paper [10] presented experimental studies of the fatigue of aluminum honeycomb structure. A block for shear tests was used for fatigue analysis, and a four-point test was used for the fatigue strength of three-layer beams with aluminum honeycomb structure [11]. Delamination between the beam layers was identified as the main type of destruction. Experimental studies showed that fatigue strength decreases with temperatures increase [12]. The fa-

tigue properties of pyramidal honeycomb structures were studied in [13], and the fatigue characteristics of multi-layer beams under the action of shear loads were studied experimentally using vibration tests in [14].

The model of fatigue characteristics was based on the concept of stiffness degradation in the paper [15]. The paper [16] studied the evolution of stiffness degradation of a multi-layer plate under the influence of fatigue loads and proposed a model for its analysis. The paper [17] showed that the stiffness degradation with increasing number of cycles was characterized by three different phases.

This paper examined the manufacturing technology of three-layer plates with honeycomb structure manufactured by additive FDM technologies. To verify the mathematical model of deformation of a three-layer plate, static experimental studies were conducted, the results of which were compared with calculated data. The obtained mathematical model was used in the simulation of fatigue tests.

In addition, a methodology for conducting fatigue tests of three-layer plates with honeycomb structure made by using additive FDM technologies was proposed. A combination of fatigue tests and numerical simulation of a three-layer plate in the ANSYS software package was implemented. As a result of calculations and experimental analysis, a *S-N* curve was constructed, and it was established that cracks in honeycomb structure were the cause of fatigue failure.

2 Methodology of fatigue tests

The purpose of this paper was to study the fatigue characteristics of three-layer plates with honeycomb structure made by using additive FDM technologies from polylactide (PLA). Fatigue properties of PLA samples made by using additive FDM technology were studied separately. The results of the study of their fatigue characteristics were used in the analysis of the fatigue characteristics of three-layer plates. It is sufficient to note that the upper and lower front layers were made of four layers of carbon fiber with stacking angles of 0, 90, 0, 90.

It is worth to add that in the following, the term "fatigue" refers to multi-cycle fatigue.

1.1 Approach to making samples

1.1.1 Samples from PLA

The design of the PLA sample is shown in Fig. 1. All dimensions in the figure are given in mm. The thickness of all samples is 6.55 mm. The samples were made using additive FDM technologies. Printing was done with PLA threads with a diameter of 0.2 mm. The printing temperature was 215 ºC, and the table temperature was 60 ºC. When printing, the threads were arranged in layers at an angle ±45° to the longitudinal axis of the sample.

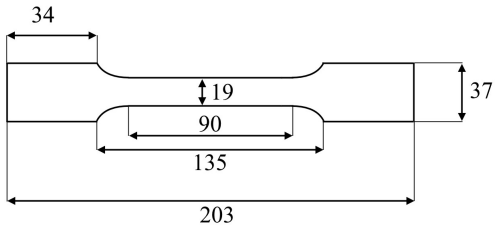

Fig. 1. Samples sketch (all dimensions are in mm)

1.1.2 Production of three-layer plates with honeycomb structure

The manufacturing technology of three-layer plates for fatigue tests consists of the following stages.

– production of honeycomb structures from PLA material using additive FDM technologies;

– production of sheathing from carbon fiber;

– gluing of a three-layer plate;

– mechanical processing of the obtained three-layer plate.

Honeycomb structure blanks with dimensions of 200×180×10 mm were made.

Carbon fiber based on SIGRAPREG C U200-0/NF-E310/30% pre-preg was chosen as the material for the sheathings. The thickness of one layer of unidirectional fabric is 0.1875 mm. The upper and lower sheathings consist of four layers of carbon-plastic with stacking angles of 0, 90, 0, 90. The layers were stacked layer-by-layer according to the scheme in the lodgment, which was vacuumed under the film, installed in the furnace and underwent polymerization. A fabric was laid on the inner and outer surfaces of the plate layer, which allowed to make the outer surface smooth, and the inner one – rough. Roughness provided increased adhesion during gluing. Plates for sheathings with dimensions of 1000×1000×0.75 mm were produced. Before the production of three-layer panels, the plate was cut on blanks with dimensions of 200×200 mm.

The gluing of the honeycomb structure with the sheathings was done with 3M™ Scotch-Weld™ DP190B/A two-component epoxy glue. The glue, the consumption of which is 450 g/m^2, was applied to the

sheathings' plates. The obtained blanks were placed in a vacuum bag on a fabric backing by the plates with the adhesive seam down, preventing the glue from flowing and ensuring the formation of grooves. The assembly was vacuumed with uniform pressing of the structure at a pressure of -0.95 atmospheres for 22 hours until strength was reached. The honeycomb structure with glued sheathing is shown in Fig. 2, a. The lower sheathing was glued similarly to the upper one. A fully glued plate is shown in Fig. 2, b. Mechanical processing was carried out using a cutting machine and a JET JSG-64 grinding machine to adjust the ends of the samples.

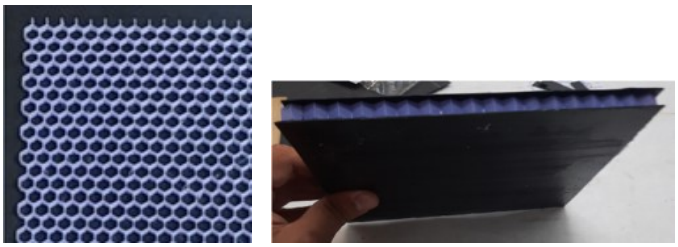

a b

Fig. 2. Gluing of a three-layer panel:
a – honeycomb structure with one sheathing;
b – three-layer panel

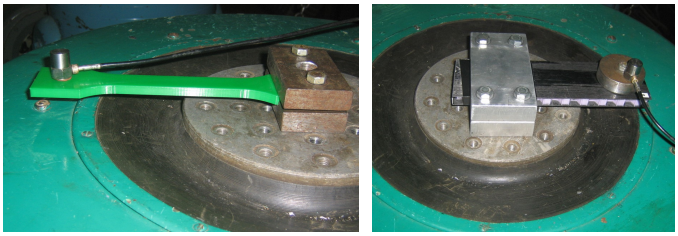

a b

Fig. 3. Photos of the samples fixed on the shaker:
a – sample from PLA; b – a three-layer plate

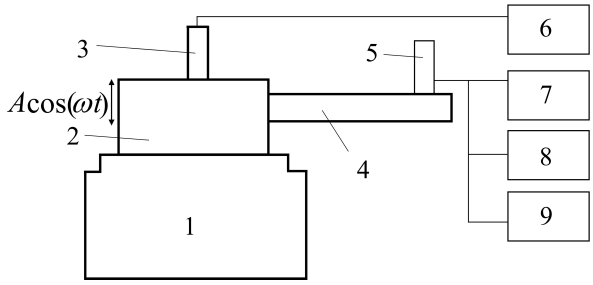

Fig. 4. Schematic diagram of the installation for fatigue tests

1.2 Methods of conducting fatigue tests

During the fatigue tests, two goals were set: the first (main one) was to investigate the fatigue of sandwich plates with honeycomb structure, which was made from PLA material using FDM technologies; the second was to study the fatigue of samples made of PLA material printed by additive FDM technologies. It is worth to emphasize that the achievement of the second goal is extremely important to achieve the first one.

Fatigue tests of three-layer plates and PLA samples were carried out using electrodynamic shakers (Fig. 3). Fig. 3, a shows a PLA sample fixed in a shaker, Fig. 3, b – a three-layer plate fixed in a shaker. The shaker reproduces periodic harmonic vertical vibrations in a wide range of excitation frequencies and amplitudes. These harmonic motions of the shaker kinematically excite elastic vibrations of three-layer plates and PLA samples. Fatigue tests are based on forced resonance vibrations of the plate. As can be seen from the experimental results below, the vibrations of three-layer plates and samples are harmonic.

Photos of the shaker for fatigue tests along with the samples are shown in Fig. 3. Samples are cantilevered. The platform of the shaker (Fig. 3) reproduces vertical harmonic vibrations, exciting the bending vibrations of the samples. Samples were fixed in this platform. During the fatigue tests, resonant vibrations of the samples were excited with the help of harmonic vibrations of fixation. A weight was attached to the free end of the three-layer plate (Fig. 3) in order for the stresses in the honeycomb structure to reach the required values.

The schematic diagram of the installation for fatigue tests is shown in Fig. 4. Its main elements are numbered. Shaker for reproduction of vibrations is indicated as 1; platform for cantilevered fixed support of the sample – 2. It is worth to emphasize that this platform carries out harmonic vibrations $A\cos(\omega t)$. The sensor mounted on the vibrator platform to measure the vibration acceleration of the fixed support is marked as 3. The tested sample is marked with the number 4, and the sensor measuring the vibration acceleration of the sample end is 5, the shaker that measures the platform vibrations is marked 6, and the free end of the sample – 7. The counter, which measures the number of cycles before the destruction of the part, is marked 8, the frequency counter, which measures the frequency of the part vibrations, is 9. At the end of the three-layer plate, a weight with a vibrator with a total mass of 257 g was installed. Firstly, it registered vibration acceleration, and secondly, its mass was selected in such a way as to obtain the required level of dynamic stresses in the honeycomb structure.

The samples were tested before their destruction. The number of vibration cycles before sample destruction was recorded. It was established that all three-layer plates were destroyed by the honeycomb structure.

For example, Fig. 5 shows a photo of the three-layer plate with a crack in the honeycomb structure, which was formed as a result of fatigue tests.

In the process of fatigue tests of a three-layer plate, there always was a change in the natural frequency of vibrations due to a decrease in the rigidity of the three-layer plate when fatigue damage occurred [17].

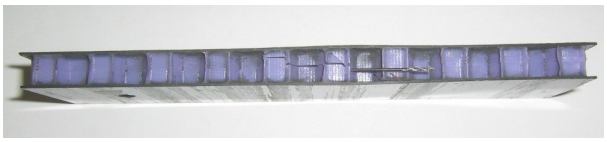

Fig. 5. Ruined honeycomb plate with a crack in the honeycomb structure

Fatigue tests of PLA samples (Fig. 1) were performed until complete destruction. At the same time, the amplitudes of vibrations of three-layer plates and PLA samples were recorded. The stress-strain state in three-layer plates and PLA samples was determined by the finite element method. Approaches to calculating the stress-strain state of structures will be considered in the following sections of the paper. According to the results of fatigue tests, *S-N* curves were constructed.

2 Approach to static tests

An approach to the experimental analysis of static deformation of three-layer plates with the honeycomb structure made by using additive FDM technologies was considered. The deformation of a cantilevered plate with one fixed edge was experimentally studied. The resulting mathematical model of the stress-strain state was used in the simulation of fatigue tests. The results of the experimental analysis will be compared.

For the tests, the TiraTest 2300 tensile machine, which allows to conduct tension and compression tests with a given traverse speed, was used. The image of the experimental stand is shown in Fig. 6, a. A wheel, which is a cylinder with a diameter of 30mm, was used to apply loads to the sample. The point of contact of the wheel was shifted from the sample edge by 15 mm. The line of contact is shown in Figure 6b. In addition, Figure 6b shows the placement scheme of deformation sensors. Strain gauges BF200-10AA-A(11)-BX30 were used to register deformation. 12 sensors were installed on each sample (Fig. 6, b).

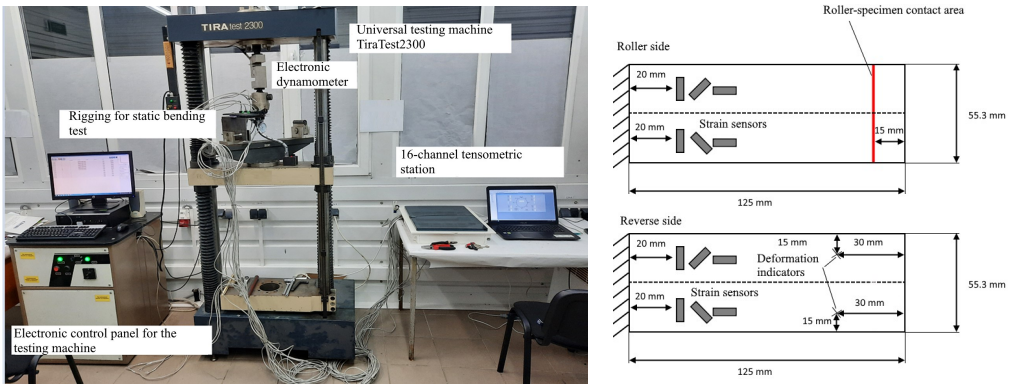

a b

Fig. 6. Experimental stand for carrying out static bending tests:
a – photo of the installation; b – diagram of deformation sensors fastening

3 Finite element modeling of experiments

When conducting fatigue tests of three-layer plates and PLA samples, a numerical analysis of the stress-strain state was carried out using finite element modeling in the ANSYS Workbench environment. The initial data for such modeling were the displacements of sample points obtained experimentally.

3.1 Modeling fatigue tests of PLA samples

To assess the stress-strain state of the samples, a dynamic finite element model was built in the ANSYS Workbench environment, which is based on a geometric model (Fig. 1). In the process of 3D printing, an edging layer with a thickness of one thread (0.2 mm) was laid along the edge of the sample. The rest of the printing area was filled layer by layer with threads at the angles ±45° relative to the longitudinal axis of the sample. As a result, the sample model consists of an edge (boundary layer) and a main part.

Orthotropic properties of materials were taken into account in the model. To model the edging layer, the orientations of the local coordinate systems of the finite elements were specified. The X axes of the local coordinate systems were directed along the tangent to the border (Fig. 7, a), the z axis was orthogonal to the print plane, and the y axis was orthogonal to the border surface.

The physical model of the sample included the properties of the materials it was made of. In particular, the edge of the sample consisted of an unidirectional layer of PLA material, the mechanical characteristics of which were as follows: density ρ=1122 kg/m^3; Young's moduli along the x, y, z axes: E_x=3.58 GPa; E_y=3.0 GPa; E_z=3.81 GPa; shear moduli G_{xy}=1.07 GPa; G_{yz}=1.41 GPa; G_{xz}=1.4 GPa; Poisson's ratio ν_{xy}=0.289; ν_{yz}=0.224; ν_{xz}=0.206. The x axis of the plastic was directed along the printing direction, the y axis was perpendicular to the x axis and lied in the printing plane, the z axis was perpendicular to the printing plane.

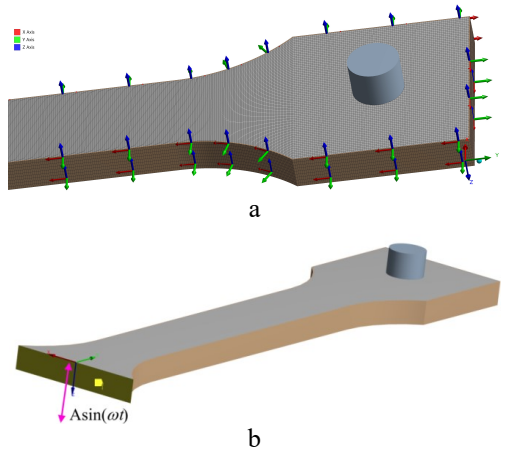

Fig. 7. Orientation of the local coordinate systems of the finite element model:
a – on the edge of the sample; b – on the main part

To evaluate the mechanical properties of the main part of the sample, the approach proposed in [18] was used. The sample was printed layer by layer, so it could be considered as a 35-layer composite structure consisting of orthotropic layers with an axis orientation of 45° in odd layers and -45° in even layers. All layers have the same thickness and consist of unidirectional PLA material, the properties of which are given above.

The method of determining the effective elastic characteristics of the sample from the described multi-layer material was considered. Hooke's law had the following form:

$$\begin{bmatrix}\sigma_{xx}\\ \sigma_{yy}\\ \sigma_{zz}\end{bmatrix}=\begin{bmatrix}\overline{C}_{11} & \overline{C}_{12} & \overline{C}_{13}\\ \overline{C}_{12} & \overline{C}_{22} & \overline{C}_{23}\\ \overline{C}_{13} & \overline{C}_{23} & \overline{C}_{33}\end{bmatrix}\cdot\begin{bmatrix}\varepsilon_{xx}\\ \varepsilon_{yy}\\ \varepsilon_{zz}\end{bmatrix}; \quad (1)$$

$$\sigma_{yz}=\overline{C}_{44}\varepsilon_{yz};\ \sigma_{xz}=\overline{C}_{55}\varepsilon_{xz};\ \sigma_{xy}=\overline{C}_{66}\varepsilon_{xy},$$

where $\overline{C}$ is the elasticity matrix of the material. Values of matrix elements $\overline{C}$ for a multi-layer sample from one material with layer orientation ±45° were defined as follows [17]:

$$\overline{c}_{ij}=\sum_{k=1}^{N}V_k c_{ij}^{(k)};(i,j)=1,2,3,6;\ \overline{c}_{pp}=\frac{1}{\Delta}\sum_{k=1}^{N}\frac{V_k}{\Delta_k}c_{pp}^{(k)};p=4.5 \quad (2)$$

where N=35 is the number of layers in the composite; V_k=1/35 is the volumetric part of the k-th layer of the composite; $C_{ij}^{(k)}$ – i,j-th element of the elasticity matrix of the k-th layer;

$$\Delta_k=C_{44}^{(k)}C_{55}^{(k)}-C_{45}^{(k)2};$$

$$\Delta=\left(\sum_{k=1}^{N}\frac{V_k}{\Delta k}C_{44}^{(k)}\right)\cdot\left(\sum_{k=1}^{N}\frac{V_k}{\Delta k}C_{55}^{(k)}\right)-\left(\sum_{k=1}^{N}\frac{V_k}{\Delta k}C_{45}^{(k)}\right)^2.$$

The elasticity matrix of the k-th layer in the axes of the sample was calculated for the considered composite as follows [17]:

$$C^{(k)}=(T^{(k)})^{\mathrm{T}}\Upsilon^{(k)}T^{(k)}, \quad (3)$$

where $T^{(k)} = \begin{bmatrix} 0.5 & 0.5 & 0 & 0 & 0 & \pm 0.5 \\ 0.5 & 0.5 & 0 & 0 & 0 & \pm 0.5 \\ 0 & 0 & 1 & 0 & 0 & 0 \\ 0 & 0 & 0 & \sqrt{0.5} & \pm\sqrt{0.5} & 0 \\ 0 & 0 & 0 & \pm\sqrt{0.5} & \sqrt{0.5} & 0 \\ \pm 1 & \pm 1 & 0 & 0 & 0 & 0 \end{bmatrix}$;

superscript for k=1, 3, 5, …, and subscript for k=2, 4, 6, …; $\Upsilon^{(k)}$ is elasticity matrix of k-th layer of the material in axes (x, y, z); the x-axis was placed along the direction of printing; the y axis lied in the printing plane perpendicular to the x axis; z axis was perpendicular to the printing plane. The values of the matrix components $\Upsilon^{(k)}$ could be calculated from the mechanical characteristics of the PLA material. The mechanical characteristics of the entire printed orthotropic sample, which are included in equation (1), were as follows: ρ=1122 kg/m^3; E_x=E_y=3.016 GPa; E_z=3.809 GPa; G_{xy}=1.232 GPa; G_{yz}=G_{xz}=1.405 GPa; ν_{xy}=0.384; ν_{yz}=ν_{xz}=0.197.

The forced vibrations of the sample under the influence of the kinematic excitation of the anchoring were simulated (Fig. 7, b). The frequency of the kinematic excitation was equal to the resonant frequency of the sample, the amplitude of the kinematic excitation was equal to the amplitude of vibrations of the shaker platform. The Harmonic Response subsystem of the ANSYS Workbench environment was used for calculations. To obtain the correct values of sample deformations, the internal friction of the material was taken into account in the model. The value of the damping factor was identified by the correspondence of the amplitude of the weight center vibrations to the values measured experimentally.

As a result of the simulation of the stress-strain state during forced vibrations, the amplitude values of the equivalent stresses according to Mises at the point of change in the curvature of the sample, at which the fracture was experimentally obtained, were calculated. As it follows from the calculations, this is the most loaded section of the sample. Based on the found amplitude values of the equivalent stresses and the experimentally obtained values of the number of cycles to destruction, the *S-N* diagram of PLA material samples was constructed.

3.2 Computational analysis of fatigue tests of three-layer plates

For the numerical simulation of the stress-strain state of sandwich plates with honeycomb structure, a finite element model that allows to calculate the stress-strain state of the plate was built. As already emphasized, the honeycomb structure was made of PLA material using additive FDM technology. To study the fatigue properties of honeycomb structure, its homogenized model was obtained, for which effective mechanical characteristics were determined [18]. This procedure is based on the finite element analysis of the static stress-strain state of the quarter cell of the honeycomb. As a result, the honeycomb structure can be replaced by a dense layer with effective elastic characteristics.

Calculation schemes of a sandwich plate with a weight are shown in Fig. 8. In particular, Fig. 8, a shows the calculation scheme, which takes into account the entire structure of the honeycomb structure (without homogenization). A sketch of the honeycomb structure is shown in Fig. 8, b. The wall thickness of the structure is equal to the double thickness of the threads (0.4 mm), that is, the wall is created in two passes of the extruder.

Finite element modeling of the three-layer plate was carried out in ANSYS Workbench. The finite element mesh includes 337505 nodes and 298961 elements. The weight was modeled as a completely rigid body, so its finite element mesh is limited by the surface of contact with the sample.

To take into account the orthotropic properties of the sheathing materials and honeycomb structure, the orientation of the local coordinate systems of the finite elements was specified. The x-axis was directed along the walls of the honeycomb structure; the y axis was perpendicular to this wall; the z axis was directed perpendicular to the printing direction.

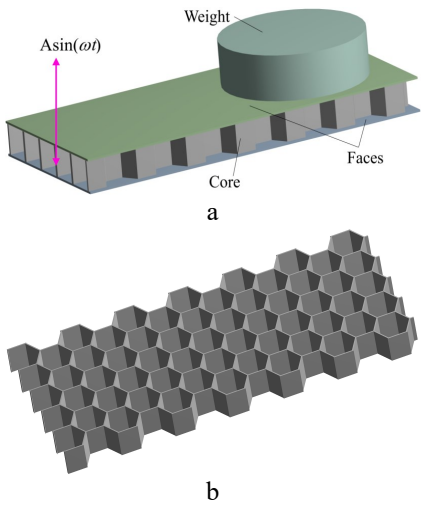

Fig. 8. Sketch of a sandwich plate with a weight: a – plate; b – a sketch of a honeycomb structure

The honeycomb structure (Fig. 8, b) consisted of unidirectional PLA material. The sheathings consisted of a four-layer composite material SIGRAPREG C U200 with alternating layer orientation 0/90/0/90. The mechanical characteristics of the sheathings were as follows: ρ=1400 kg/m^3; E_x=E_y=35 GPa; E_z=8 GPa; G_{xy}=6 GPa; G_{yz}=G_{xz}=30 GPa; ν_{xy}=0.01; ν_{yz}=ν_{xz}=0.09.

The mechanical characteristics of the homogenized dense layer of the honeycomb structure were obtained using finite element modeling according to the method described in [18]. The mechanical characteristics of the homogenized orthotropic layer were as follows: ρ=89 kg/m^3; E_x=E_y=2.16 MPa; E_z=272.67 MPa; G_{xy}=0.84 MPa; G_{yz}=G_{xz}=52.28 MPa; ν_{xy}=0.98; ν_{yz}=0.00166; ν_{xz}=0.00184.

The analysis of the harmonic response of the finite element model of the three-layer plate was carried out under the influence of the kinematic excitation of the anchoring (Fig. 7, b). The frequency of the disturbing load ω was equal to the natural frequency of the structure of 124.59 Hz. Amplitude A was equal to the amplitude of vibrations of the shaker. In the finite element model of vibrations, material damping according to the Rayleigh model was taken into account. The value of the damping factor was identified from the condition of matching the amplitudes of the weight center vibrations obtained by calculation and in the experimental study. As a result of the calculation of linear forced vibrations, the amplitudes of vibrations of equivalent stresses were determined.

Based on the amplitude values of the equivalent stresses found from the homogenized model and the experimentally obtained values of the number of cycles to destruction of the three-layer plates, a *S*-*N* curve was constructed.

4 Test results

The calculation of the static deformation of three-layer plates was carried out on the basis of the computer models described in section 4.2. A force was applied to the upper sheathing of the plate, which describes the action of the wheel (Fig. 6, b). The value of force F was determined from experimental data.

A comparison of the results of calculation of deformations at the points of placement of strain gauges and the sensors readings was made. Based on these results, conclusions were made about the correspondence of the calculation model of the three-layer plate to its static behavior, and the properties of the plate's static deformation were analyzed. In the stressed state of the plate, longitudinal deformations ε_{xx} prevail.

In Fig. 9, the solid line shows the results of calculating the static deformations of the plate depending on the applied transverse force F. In the same figure, the experimental values of the longitudinal deformations of the plate are shown in dots. In the experiments, brittle destruction of the samples was observed. To calculate the longitudinal deformations shown in Fig. 9, a finite element model of honeycomb structure without homogenization was used. Immediately after the last point with maximum deformations (Fig. 9), brittle destruction of the sample was observed.

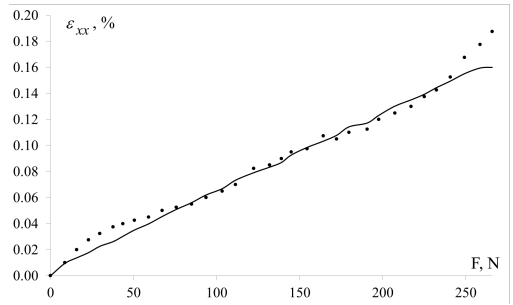

Fig. 9. Longitudinal static deformations of three-layer plates

Thus, a comparison of the experimental static response and the results of finite element modeling showed that both the sandwich plate model with an accurate finite element description of the honeycomb structure and the homogenized model adequately describe the behavior of the sample.

16 samples were made for fatigue tests. Fig. 1 shows a sample sketch. Fatigue tests were carried out according to the methodology given in section 1.2.

For each sample, the resonance frequency was determined by experimental obtaining of the frequency response. For this, the frequency of the external influence (frequency of vibration of the shaker platform) was changed with a constant amplitude of this influence. The natural frequencies of vibrations of the samples are given in the second row of the Table 1 in Hz. The serial number of the sample is indicated in the first line of this table. As follows from this table, all natural frequencies are in the range 30–32 Hz. Samples no. 1 and 5 are not considered because they were found to be defective before the fatigue tests began.

During the fatigue tests, the number of cycles before destruction of the samples N was recorded. The destructions were observed in the most loaded place in the section of the circular transition. Finite element modeling was used to determine the value of the amplitude of vibrations of the equivalent stresses in this area. For this, the approach discussed in section 3.1 was applied. Amplitudes of equivalent stresses in the

sample are given in the fourth row of the Table 1. The number of cycles before sample failure is indicated in the third line. It should be noted that the third and eighth samples did not collapse (Table 1) due to the fact that the amplitude stress values are smaller than the endurance limit.

Table 1. Sample destruction parameters

Sample number	1	2	3	4	5	6	7	8	9	10	11	12	13	14	15	16
The value f the natural frequency, Hz	30.0	32.0	31.0	30.0	31.0	31.5	31.9	30.2	31.2	31.0	30.0	30.0	32.0	32.6	31.6	31.8
Number of cycles to destruction, $N\cdot10^{-3}$	–	327	>11000	238	–	2283	4930	>11000	62	63	2068	257	865	5670	73	2520
The amplitude of the equivalent stress, σ_{max}, MPa	–	15.62	7.52	16.95	–	13.11	11.27	8.47	24.87	25.57	13.26	19.80	16.20	10.21	21.59	10.78

The use of a vibrometer in the experimental scheme of fatigue tests (Fig. 4) made it possible to study the spectral densities of vibrations of the cantilevered end of the samples. A characteristic view of the amplitude spectra of the dynamic response of the sample is shown in Fig. 10, a. As can be seen from this figure, the vibrations of the end of the samples are monoharmonic.

The Table 1 was used to construct a *S-N* curve. The results of the experimental analysis that are given in the Table 1, are shown in Fig. 10, b with points. The figure shows the dependence of the amplitude of the equivalent stresses in the most loaded section of the sample on the number of cycles to failure. The obtained points were approximated by the method of least squares. The following equation was used to approximate the *S-N* curve. The Table 1 was used to construct a *S-N* curve. The results of the experimental analysis that are given in the Table 1, are shown in Fig. 10, b with points. The figure shows the dependence of the amplitude of the equivalent stresses in the most loaded section of the sample on the number of cycles to failure. The obtained points were approximated by the method of least squares. The following equation was used to approximate the *S-N* curve:

$$\sigma_{\max}^{m} N = C, \qquad (4)$$

where m and C are fatigue curve parameters. The application of the method of least squares made it possible to find the parameters m and C: m=5.166; log$C$=42.91. Curve (4) is shown in Fig. 10, b with a solid line. The endurance limit of the material was found experimentally: σ_{-1}=11 МПа.

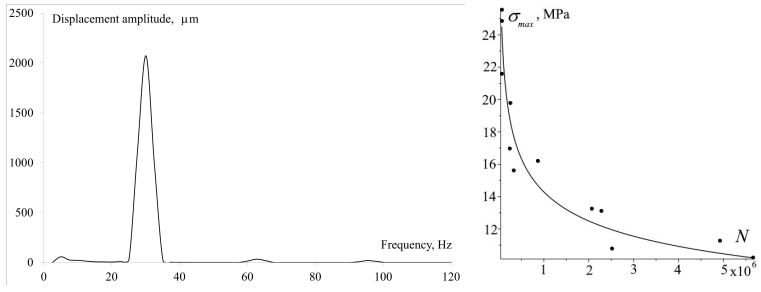

a b

Fig. 10. Characteristics of fatigue tests:
a – spectral densities of the dynamic response of the end of the PLA sample; b – *S-N* curve

Fatigue tests of sandwich plates were carried out on 12 samples. The geometry of sandwich plates is shown in Fig. 8a. The entire honeycomb structure is shown in Fig. 8, b.

Resonance vibrations of sandwich plates were studied. With the use of frequency responses, the natural frequencies of bending vibrations of all sandwich plates, which are listed in the Table 2, were found; the first natural frequency was in the frequency range of 109–138 Hz. A finite element calculation of natural frequencies of the considered sandwich plate was carried out. From the calculation of natural frequencies taking into account the exact model of the honeycomb structure (without homogenization), it follows that the first natural frequency was equal to 124.59 Hz. From the calculation of a sandwich plate with homogenized structure, the first natural frequency of 123.89 Hz was obtained. These natural frequencies correspond well to the experimental data (Table 2).

With the help of a shaker, which is included in the scheme of fatigue tests, the spectral densities of the dynamic response of the end of the cantilevered plate were studied. For example, Fig. 11, a shows the spectral densities of the dynamic response of sample no. 9. Thus, the vibrations of the end of the sandwich plate were close to monoharmonic.

Table 2. Natural frequencies of 12 sandwich plates

Sample number	1	2	3	4	5	6	7	8	9	10	11	12
The value of the natural frequency, Hz	128	138	136	130	125	122	121.6	120	109	110	129	133
Natural frequency after the occurrence of the first defect	126.0	–	134.0	129.0	123.0	119.0	105.0	–	107.0	108.0	126.0	131.0

During the fatigue tests, two values of the number of vibration cycles were recorded: the number of vibration cycles before sample destruction N_t and the number of cycles before the first change in natural frequency N_c. The latter is associated with a decrease in the stiffness of the sandwich plate, which is due to the occurrence of fatigue damage. The values of natural frequencies after their first changes are shown in the bottom row of the Table 2.

The destruction of sandwich plates occurred only in the layer of honeycomb structure. The stress values in the honeycomb structure were estimated according to the computational method described in section 3.2. Table 3 shows the results of the experimental analysis of the samples and the calculation of the amplitudes of the equivalent stresses in the honeycomb structure. The first column of the table shows the sample number, the second column shows the number of cycles before sample destruction N_t, the third column shows the amplitudes of the equivalent stresses in the honeycomb structure $\overline{\sigma}_{max}$, obtained according to the homogenized model, the fourth column shows the number of cycles of fatigue tests before the first change in natural frequency N_c, fifth one - the equivalent stresses obtained from the exact model of the honeycomb structure. The results of the finite element analysis showed that the longitudinal walls of the structure were mostly loaded. The distribution of equivalent stresses was extremely uneven. Many cycles passed from the change of the natural frequency of vibrations to the destruction of the sample. The values of natural frequencies before and after their changes are given in the Table 3. For most samples, the natural frequency changed by 2–3 Hz. An exception is sample no. 7, in which a significant change in natural frequency was observed.

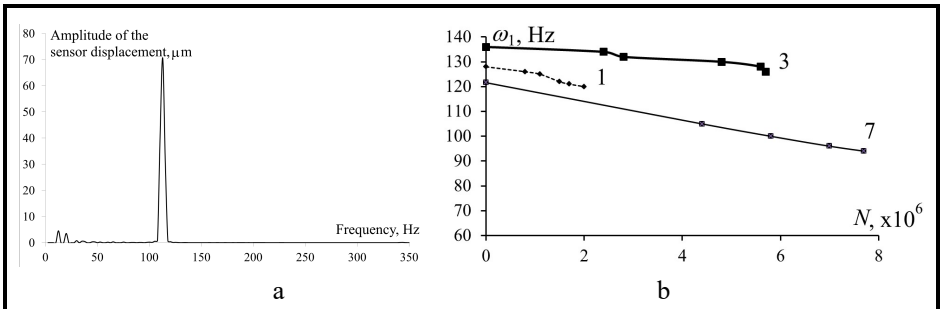

Fig. 11. Vibrations characteristics of sandwich plates
a – spectral densities of the sample response;
b – dependence of the first natural frequencies of the samples on the number of cycles

Table 3. Results of fatigue tests of sandwich plate samples

Sample number	$N_t \cdot 10^{-3}$	$\overline{\sigma}_{max}$, MPa	$N_c \cdot 10^{-3}$	σ^*_{max}, MPa	Defects in the destroyed sample
1	2130	0.223	800	6.815	The sample has a crack in the honeycomb
2	>11000	0.155	>11000	2.730	Sample without defects
3	6470	0.148	2400	4.567	The sample has a crack in the honeycomb
4	316	0.288	96	8.937	The sample has a crack in the honeycomb and folding of the honeycomb wall
5	1090	0.236	400	6.318	The sample has a crack in the honeycomb and folding of the honeycomb wall
6	86	0.542	64	13.400	The sample has a crack in the honeycomb
7	8900	0.203	4400	4.920	The sample has a crack in the honeycomb
8	>11000	0.143	>11000	2.410	Sample without defects
9	102	0.449	40	11.504	The sample has a crack in the honeycomb
10	124	0.309	50	8.302	The sample has a crack in the honeycomb
11	3710	0.217	1500	6.605	The sample has a crack in the honeycomb and delamination of the carbon fiber
12	8650	0.194	3500	4.713	The sample has a crack in the honeycomb

It should be noted that a change in the natural frequency of the sample during fatigue tests shows the occurrence of a defect in the sample. As it was emphasized, it was observed in all studied samples. Fig. 11, b shows the dependence of the first natural frequencies of sandwich plate samples 1, 3, 7 on the number of cycles. After the first change, a further decrease in natural frequencies, which was accompanied by an increase in the defectiveness of the samples, was observed.

The *S-N* diagram, in which the number of cycles before the change of the natural frequency N_c was laid along the abscissa axis, was considered. This diagram was calculated using the S-N diagram of PLA material (Fig. 10, b). After calculating the maximum stresses in the honeycomb structure of the sandwich plate according to the diagram (Fig. 10, b), the number of cycles N_c was determined. The results of such analysis are shown by a solid line in Fig. 13, a. The dots show the experimental results from Table 3. The calculated and experimental results are close.

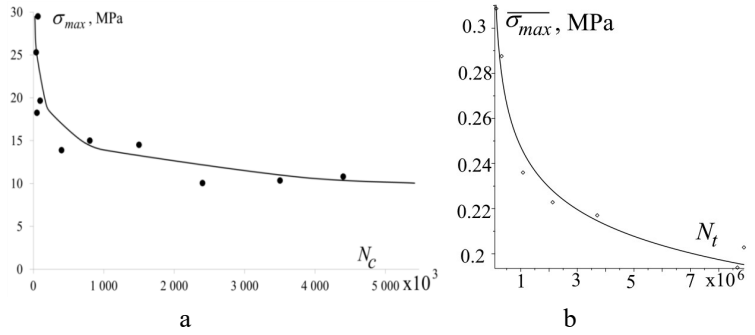

Fig. 13. S-N curves of plates:
a – the number of cycles until the first change in natural frequency is laid along the abscissa axis; b – the number of cycles until the destruction of the honeycomb structure is laid along the abscissa axis

The *S-N* diagram, in which the number of cycles before the destruction of the sample will be given along the abscissa axis, was considered. Amplitudes of equivalent stresses were determined from the homogenized model of the honeycomb structure. The method of calculating equivalent stresses is considered in section 3.2. The *S-N* diagram of honeycomb plates is shown in Fig. 13, b. The solid line in the figure shows the approximation in the form (4) of the *S-N* diagram. This approximation was obtained by the method of least squares. The constants m and C acquire value for it: m=9.21; log(C)=55.67.

After the destruction of the sandwich plates, the defects were analyzed. Ultrasonic control and X-ray were applied. With the help of ultrasonic control, delamination between layers of carbon fiber, lack of gluing between the honeycomb and sheathing and cracks in the walls of the structure could be detected, which is possible only if their characteristic size was greater than 20 mm. X-ray method is more sensitive. It allows to detect internal cracks in the walls of the structure and the absence of gluing of much smaller sizes. An X-ray also allows to register the crumpling of the cells. At the same time, it is necessary to carry out a special analysis of X-ray images, which have previously been digitized and subjected to binary transformation.

The results of the analysis of defects in the samples are given in the last column of the Table 3. It should be noted that no defects were found in the samples that were not destroyed. In most of the samples, only cracks in the walls of the structure were found. In two samples, in addition to cracks in the structure, crumpling of the cells was found, in one sample - both cracks in the structure and delamination between the layers of carbon fiber.

Conclusions

The paper studies the fatigue of composite sandwich plates with honeycomb structure made of PLA, manufactured using additive FDM technologies. The upper and lower layers of the sandwich plates are made of four-layer composite material SIGRAPREG C U200 with alternating layer orientation 0/90/0/90.

An approach to the study of sandwich plate fatigue based on resonant vibration tests of sandwich plates is proposed. During the test, the plate performs forced linear bending monoharmonic resonant vibrations. The vibration acceleration of the free end of the cantilevered plate is analyzed and the number of cycles before the destruction of the honeycomb structure is determined. The *S-N* diagram is studied. It is shown that it is described by a typical power dependence, which is used for *S-N* diagrams of metals such as steel and aluminum.

Fatigue tests of sandwich plates are accompanied by a change in natural frequencies due to the occurrence of defects in the plate. After that, the plate does not break and withstands a significant number of cycles before breaking. With an increase in the number of cycles, a gradual decrease in the first natural frequency of sandwich plates is observed due to a decrease in rigidity and accumulation of defects in the samples.

The *S-N* diagram of sandwich plates before changing their natural vibration frequency is studied. It is shown that such a diagram can be predicted by a numerical calculation based on the *S-N* diagram of the PLA material.

Financing

The research was funded by the National Research Fund of Ukraine (grant 128/02.2020).

References

1. Matthews, N. (2018). Additive metal technologies for aerospace sustainment. *Aircraft Sustainment and Repair*, pp. 845–862. https://doi.org/10.1016/B978-0-08-100540-8.00015-7.
2. Boparai, K. S. & Singh, R. (2017). Advances in fused deposition modeling. *Reference Module in Materials Science and Materials Engineering*. https://doi.org/10.1016/B978-0-12-803581-8.04166-7.
3. Xu, M., Liu, D., Wang, P., Zhang, Z., Jia, H., Lei, H., & Fang, D. (2020). In-plane compression behavior of hybrid honeycomb metastructures: Theoretical and experimental studies. *Aerospace Science and Technology*, vol. 106, paper ID 106081. https://doi.org/10.1016/j.ast.2020.106081.
4. Chen, Y., Li, T., Jia, Z., Scarpa, F., Yao, C., & Wang, L. (2018). 3D printed hierarchical honeycombs with shape integrity under large compressive deformations. *Materials and Design*, vol. 137, pp. 226–234. https://doi.org/10.1016/j.matdes.2017.10.028.
5. Parsons, E. M. (2019). Lightweight cellular metal composites with zero and tunable thermal expansion enabled by ultrasonic additive manufacturing: Modeling, manufacturing, and testing. *Composite Structures*, vol. 223, paper ID 110656. https://doi.org/10.1016/j.compstruct.2019.02.031.
6. Abbadi, A., Tixier, C., Gilgert, J., & Azari, Z. (2015). Experimental study on the fatigue behaviour of honeycomb sandwich panels with artificial defects. *Composite Structures*, vol. 120, pp. 394–405. https://doi.org/10.1016/j.compstruct.2014.10.020.
7. Belingardi, G., Martella, P., & Peroni, L. (2007). Fatigue analysis of honeycomb-composite sandwich beams. *Composites Part A: Applied Science and Manufacturing*, vol. 38, iss. 4, pp. 1183–1191. https://doi.org/10.1016/j.compositesa.2006.06.007.
8. Belouettar, S., Abbadi, A., Azari, Z., Belouettar, R. & Freres, P. (2009). Experimental investigation of static and fatigue behaviour of composites honeycomb materials using four point bending tests. *Composite Structures*, vol. 87, iss. 3, pp. 265–273. https://doi.org/10.1016/j.compstruct.2008.01.015.
9. Jen, Y.-M., Ko, C.-W., & Lin, H.-B. (2009). Effect of the amount of adhesive on the bending fatigue strength of adhesively bonded aluminum honeycomb sandwich beams. *International Journal of Fatigue*, vol. 31, iss. 3, pp. 455–462. https://doi.org/10.1016/j.ijfatigue.2008.07.008.
10. Bianchi, G., Aglietti, G. S., & Richardson, G. (2012). Static and fatigue behaviour of hexagonal honeycomb cores under in-plane shear loads. *Applied Composite Materials*, vol. 19, pp. 97–115. https://doi.org/10.1007/s10443-010-9184-5.
11. Jen, Y.-M. & Chang, L.-Y. (2008). Evaluating bending fatigue strength of aluminum honeycomb sandwich beams using local parameters. *International Journal of Fatigue*, vol. 30, iss. 6, pp. 1103–1114. https://doi.org/10.1016/j.ijfatigue.2007.08.006.
12. Jen, Y.-M. & Lin, H.-B. (2013). Temperature-dependent monotonic and fatigue bending strengths of adhesively bonded aluminum honeycomb sandwich beams. *Materials and Design*, vol. 45, pp. 393–406. https://doi.org/10.1016/j.matdes.2012.09.028.
13. Cote, F., Fleck, N. A., & Deshpande, V. S. (2007). Fatigue performance of sandwich beams with a pyramidal core. *International Journal of Fatigue*, vol. 29, iss. 8, pp. 1402–1412. https://doi.org/10.1016/j.ijfatigue.2006.11.013.
14. Burman, M. & Zenkert, D. (2000). Fatigue of undamaged and damaged honeycomb sandwich beams. *Journal of Sandwich Structures and Materials*, vol. 2, iss. 1, pp. 50–74. https://doi.org/10.1177/109963620000200103.
15. Abbadi, A., Azari, Z., Belouettar, S., Gilgert, J., & Freres, P. (2010). Modelling the fatigue behaviour of composites honeycomb materials (aluminium/aramide fibre core) using four-point bending tests. *International Journal of Fatigue*, vol. 32, iss. 11, pp. 1739–1747. https://doi.org/10.1016/j.ijfatigue.2010.01.005.
16. Whitworth, H. A. (1998). A stiffness degradation model for composite laminates under fatigue loading. *Composite Structures*, vol. 40, iss. 2, pp. 95–101. https://doi.org/10.1016/S0263-8223(97)00142-6.
17. Boukharouba, W., Bezazi, A., & Scarpa, F. (2014). Identification and prediction of cyclic fatigue behavior in sandwich panels. *Measurement*, vol. 53, pp. 161–170. https://doi.org/10.1016/j.measurement.2014.03.041.
18. Catapano, A. & Montemurro, M. (2014). A multi-scale approach for the optimum design of sandwich plates with honeycomb core. Part I: homogenisation of core properties. *Composite Structures*, vol. 118, pp. 664–676. https://doi.org/10.1016/j.compstruct.2014.07.057.

Received 11 May 2022

Багатоциклова втома композитних тришарових пластин зі стільниковими заповнювачами, які виготовлено адитивними технологіями FDM

[1] Б. В. Успенський, [2] І. І. Деревянко, [1, 3, 4] К. В. Аврамов, [1] О. Ф. Поліщук, [5] О. Ф. Саленко

[1] Інститут проблем машинобудування ім. А. М. Підгорного НАН України, 61046, Україна, м. Харків, вул. Пожарського, 2/10

[2] Державне підприємство «Конструкторське бюро «Південне» ім. М. К. Янгеля», 49008, Україна, м. Дніпро, вул. Криворізька, 3

[3] Харківський національний університет радіоелектроніки, 61166, Україна, м. Харків, пр. Науки, 14

[4] Національний аерокосмічний університет «Харківський авіаційний інститут» ім. М. Є. Жуковського, 61070, м. Харків, вул. Чкалова, 17

[5] Національний технічний університет України «Київський політехнічний інститут імені Ігоря Сікорського», 03056, Україна, м. Київ, пр. Перемоги, 37

Розглянуто багатоциклову втому тришарових пластин зі стільниковим заповнювачем, який виготовлено за допомогою адитивних технологій FDM з полілактиду. Як матеріал для верхніх і нижніх обкладинок обрано вуглепластик на базі препрегу марки SIGRAPREG C U200-0/NF-E310/30%. Аналіз втоми тришарових пластин зі стільниковим заповнювачем спирається на їх вібраційні випробування. Для дослідження втомних характеристик полілактиду стільникових заповнювачів виготовлено спеціальні зразки. Втомні характеристики заповнювачів досліджено на тришарових зразках із використанням вуглепластикових обшивок Експеримент супроводжувався скінченно-елементним моделюванням втомних випробувань у програмному комплексі ANSYS. Вивчено втомні властивості тришарових пластин.

***Ключові слова**: стільниковий заповнювач, адитивна технологія FDM, тришарові пластини, втомні випробування, діаграма Веллера.*

Література

1. Matthews N. Additive metal technologies for aerospace sustainment. *Aircraft Sustainment and Repair*. 2018. P. 845–862. https://doi.org/10.1016/B978-0-08-100540-8.00015-7.
2. Boparai K. S., Singh R. Advances in fused deposition modeling. *Reference Module in Materials Science and Materials Engineering*. 2017. https://doi.org/10.1016/B978-0-12-803581-8.04166-7.
3. Xu M., Liu D., Wang P., Zhang Z., Jia H., Lei H., Fang D. In-plane compression behavior of hybrid honeycomb metastructures: Theoretical and experimental studies. *Aerospace Science and Technology*. 2020. Vol. 106. Paper ID 106081. https://doi.org/10.1016/j.ast.2020.106081.
4. Chen Y., Li T., Jia Z., Scarpa F., Yao C., Wang L. 3D printed hierarchical honeycombs with shape integrity under large compressive deformations. *Materials and Design*. 2018. Vol. 137. P. 226–234. https://doi.org/10.1016/j.matdes.2017.10.028.
5. Parsons E. M. Lightweight cellular metal composites with zero and tunable thermal expansion enabled by ultrasonic additive manufacturing: Modeling, manufacturing, and testing. *Composite Structures.* 2019. Vol. 223. Paper ID 110656. https://doi.org/10.1016/j.compstruct.2019.02.031.
6. Abbadi A., Tixier C., Gilgert J., Azari Z. Experimental study on the fatigue behaviour of honeycomb sandwich panels with artificial defects. *Composite Structures*. 2015. Vol. 120. P. 394–405. https://doi.org/10.1016/j.compstruct.2014.10.020.
7. Belingardi G., Martella P., Peroni L. Fatigue analysis of honeycomb-composite sandwich beams. *Composites Part A: Applied Science and Manufacturing*. 2007. Vol. 38. Iss. 4. P. 1183–1191. https://doi.org/10.1016/j.compositesa.2006.06.007.
8. Belouettar S., Abbadi A., Azari Z., Belouettar R., Freres P. Experimental investigation of static and fatigue behaviour of composites honeycomb materials using four point bending tests. *Composite Structures*. 2009. Vol. 87. Iss. 3. P. 265–273. https://doi.org/10.1016/j.compstruct.2008.01.015.
9. Jen Y.-M., Ko C.-W., Lin H.-B. Effect of the amount of adhesive on the bending fatigue strength of adhesively bonded aluminum honeycomb sandwich beams. *International Journal of Fatigue*. 2009. Vol. 31. Iss. 3. P. 455–462. https://doi.org/10.1016/j.ijfatigue.2008.07.008.
10. Bianchi G., Aglietti G. S., Richardson G. Static and fatigue behaviour of hexagonal honeycomb cores under in-plane shear loads. *Applied Composite Materials*. 2012. Vol. 19. P. 97–115. https://doi.org/10.1007/s10443-010-9184-5.

11. Jen Y.-M., Chang L.-Y. Evaluating bending fatigue strength of aluminum honeycomb sandwich beams using local parameters. *International Journal of Fatigue*. 2008. Vol. 30. Iss. 6. P. 1103–1114. https://doi.org/10.1016/j.ijfatigue.2007.08.006.
12. Jen Y.-M., Lin H.-B. Temperature-dependent monotonic and fatigue bending strengths of adhesively bonded aluminum honeycomb sandwich beams. *Materials and Design*. 2013. Vol. 45. P. 393–406. https://doi.org/10.1016/j.matdes.2012.09.028.
13. Cote F., Fleck N. A., Deshpande V. S. Fatigue performance of sandwich beams with a pyramidal core. *International Journal of Fatigue*. 2007. Vol. 29. Iss. 8. P. 1402–1412. https://doi.org/10.1016/j.ijfatigue.2006.11.013.
14. Burman M., Zenkert D. Fatigue of undamaged and damaged honeycomb sandwich beams. *Journal of Sandwich Structures and Materials*. 2000. Vol. 2. Iss. 1. P. 50–74. https://doi.org/10.1177/109963620000200103.
15. Abbadi A., Azari Z., Belouettar S., Gilgert J., Freres P. Modelling the fatigue behaviour of composites honeycomb materials (aluminium/aramide fibre core) using four-point bending tests. *International Journal of Fatigue*. 2010. Vol. 32. Iss. 11. P. 1739–1747. https://doi.org/10.1016/j.ijfatigue.2010.01.005.
16. Whitworth H. A. A stiffness degradation model for composite laminates under fatigue loading. *Composite Structures*. 1998. Vol. 40. Iss. 2. P. 95–101. https://doi.org/10.1016/S0263-8223(97)00142-6.
17. Boukharouba W., Bezazi A., Scarpa F. Identification and prediction of cyclic fatigue behavior in sandwich panels. *Measurement*. 2014. Vol. 53. P. 161–170. https://doi.org/10.1016/j.measurement.2014.03.041.
18. Catapano A., Montemurro M. A multi-scale approach for the optimum design of sandwich plates with honeycomb core. Part I: homogenisation of core properties. *Composite Structures*. 2014. Vol. 118. P. 664–676. https://doi.org/10.1016/j.compstruct.2014.07.057.